PHYSICS AND CHEMISTRY OF SOLID STATE
V. 26, No. 4 (2025) pp. 774-780
Section: Physics

DOI: 10.15330/pcss.26.4.774-780

Vasyl Stefanyk Carpathian National University

ФІЗИКА І ХІМІЯ ТВЕРДОГО ТІЛА
Т. 26, № 4 (2025) С. 774-780
Фізико-математичні науки

PACS: 61.50.Ks, 64.60.i, 68.35.Rh, 82.80.Ej, 82.45.Gj

ISSN 1729-4428 (Print)
ISSN 2309-8589 (Online)

M. V. Chekailo[1], S. I. Yushchuk[1], S. O. Yuryev[1], L. G. Akselrud[2], V. V. Mokliak[3,4]

Phase Transitions in Ag_8SnSe_6 and Ag_8SnS_6: Mössbauer and X-ray Study

[1]*National University ''Lviv Polytechnic", Department of Physics, Lviv, Ukraine, serhii.o.yuriev@lpnu.ua, mykola.v.chekailo@lpnu.ua;*
[2]*Ivan Franko National University of Lviv, Department of Inorganic Chemistry, Lviv, Ukraine, lev.akselrud@lnu.edu.ua;*
[3]*G.V. Kurdyumov Institute for Metal Physics, N.A.S. of Ukraine, Kyiv, Ukraine, mvvmcv@gmail.com;*
[4]*Ivano-Frankivsk National Technical University of Oil and Gas, Ivano-Frankivsk, Ukraine, volodymyr.mokliak@nung.edu.ua*

The structural transformations accompanying the low-temperature phase transition (PT) β′→γ in the argyrodite Ag_8SnSe_6 characterized by mixed electron-ionic conductivity, have been studied using nuclear gamma resonance (NGR) and X-ray diffraction (XRD). Parallel Mössbauer studies were performed on the structurally related canfieldite Ag_8SnS_6. An abrupt decrease in the probability of the Mössbauer effect and isomer shifts was observed in argyrodite and canfieldite near 356 K and 445 K, respectively, corresponding to phase transitions in these compounds. Spatial models of the first and second coordination spheres of Ag_8SnSe_6 in the β′ and γ-modifications have been proposed.

Keywords: argyrodite, canfieldite, phase transitions, superionic conductors.

Received 20 May 2025; Accepted 26 November 2025.

Introduction

Significant interest has been shown in solid-state materials exhibiting high ionic and mixed electronic-ionic conductivity, which are referred to as superionic conductors or solid electrolytes (SE) [1]. The high ionic conductivity of solid electrolytes is attributed to the presence of ordering in their crystal lattices, which can be classified as follows: (1) intrinsic ordering, including Schottky and Frenkel defects as well as radiation-induced defects; (2) impurity ordering caused by foreign atoms; and (3) structural ordering [2]. Ions located in partially occupied sites of the structurally ordered crystal lattice of solid electrolytes are capable of moving through crystallographic channels through crystallographic channels that form one-, two-, or three-dimensional networks which facilitate their high ionic mobility [3, 4]. Practical interest in solid electrolytes arises from the possibility of creating heterophase structures based on them, such as solid electrolyte–metal and solid electrolyte–semiconductor interfaces. These heterostructures serve as the foundation for new functional elements, including high-capacitance capacitors, optoelectronic electrochromic devices, solid-state batteries (such as ion-conducting glass), FLASH memory elements, and others [5, 6, 7, 8, 9]. Such materials also exhibit unique photocatalytic and thermoelectric properties [10, 11].

The compound Ag_8SnSe_6 belongs to the subgroup of ternary chalcogenides with the general formula $A^I_8B^{IV}X_6$ (A^I = Cu, Ag; B^{IV} = Si, Ge, Sn; X = S, Se, Te). This subgroup, in turn, belongs to a rather broad group of compounds which were first described by W.F. Kuhs et al. [12] with the general formula $A^{m+}_{(12-\ n-\ x)/m}B^{n+}X^{2-}_{6-x}Y^-_x$ (A: Cu, Ag, Cd, Hg; B: Ga, Si, Ge, Sn, P, As; X= S, Se, Te; Y=Cl, Br, I; $0 \le x \le 1$) [13]. All these compounds exhibit quite interesting common features. First and foremost, they demonstrate polymorphism. The phase transition temperatures of ternary chalcogenides are close to room temperature and can vary from 325 K for Ag_8GeTe_6 to 507 K for Ag_8SiS_6 [14]. In the high-temperature crystalline phase, they possess a face-centered cubic lattice (space group $F\bar{4}3m$) with an ordered cation sublattice A. This, in turn, creates conditions for the

existence of ionic conductivity. The group of compounds Ag_8SnX_6 (X = S, Se) belongs to materials with mixed conductivity.

The aim of this work is to investigate the structural transformations associated with the phase transition β′→γ in argyrodite Ag_8SnSe_6 and the phase transition α″→γ in the structurally related canfieldite Ag_8SnS_6, employing Mössbauer spectroscopy and X- ray structural analysis.

I. Preparation and methods of study of Ag_8SnSe_6 and Ag_8SnS_6 compounds

The compound Ag_8SnSe_6 was synthesized via a solid-state reaction from chemically pure elemental substances. Stoichiometric amounts of Ag (99.999%), Sn (99.999%), and Se (99.999%) were placed into a quartz ampoule, which was evacuated to a pressure not worse than 10^{-3} Pa and then sealed. The ampoule containing the charge was placed in the center of a resistive furnace and slowly heated to the point of direct melting. The synthesis of the compounds was carried out in detail according to the method described in [15, 16] From the obtained polycrystalline materials, block-shaped single crystals with linear dimensions up to 4 mm were grown by the pseudo-sublimation method. Crystals obtained from the same batch were used for structural and Mössbauer studies.

Mössbauer spectra of Sn-119 nuclei were recorded using a nuclear gamma resonance spectrometer operating in the constant acceleration mode. $CaSn^{119m}O_3$ served as the gamma-ray source, maintained at a temperature of 295 K. Calibration of the Mössbauer spectra was performed using the spectra of α-Fe_2O_3 and SnO_2. The instrumental linewidth was equal to $G_{1/2}$ = 0.65 mm/s. Samples of Ag_8SnSe_6 and Ag_8SnS_6 with a thickness of 0.1 mg/cm^2 based on Sn^{119}, were placed in a vacuum furnace where the temperature during measurements was varied from 295 K to 700 K. Temperature stabilization was maintained with an accuracy of ±0.2 K. The Mössbauer spectra were analyzed assuming Lorentzian line shapes for the resonance lines.

X-ray structural studies before and after the β′→γ phase transition in argyrodite were conducted using X-ray diffractometer. For temperature-dependent diffraction measurements, powdered samples were placed in a vacuum-sealed thermal chamber. Temperature stabilization was maintained with an accuracy of ±0.05 K. Experimental data arrays in the format of intensity versus 2θ angle were obtained using the step-scan method (step size of 0.03° in 2θ scale with a counting time of 10–15 s per point) and Cu Kα radiation. The crystal structure type was determined based on plausible structural models of the argyrodite lattice. Refinement of the structural parameters was performed using experimental data arrays of intensity versus 2θ angle obtained from X-ray measurements, applying the Rietveld method with the WinCSD software package [17].

II. Results and discussion

2.1. Diffractograms of Ag_8SnSe_6 argyrodite and its structure parameters.

X-ray diffraction patterns of powdered Ag_8SnSe_6 were recorded at 295 K and 393 K (Fig. 1 and 2). The crystallographic parameters of the β′ and γ - phases of Ag_8SnSe_6 were determined from these diffraction patterns (Tables 1 and 2) [18]. Sn atoms in the γ phase of Ag_8SnSe_6 are located at the centers of regular tetrahedra coordinated by four Se atoms, whereas in the β′ phase of Ag_8SnSe_6, the tetrahedra are distorted, as evidenced by differences in Se–Sn–Se bond lengths and angles (Table 2). The deformation parameters calculated following the method [19] described in for bond lengths (σ_l) and bond angles (σ_θ) are 0.042 Å and 2.60°, respectively.

2.2. Mössbauer effect on Sn^{119} in argyrodite and canfieldite in the in the vicinity of phase transitions

Figs. 3 and 4 show the Sn-119 Mössbauer spectra of argyrodite Ag_8SnSe_6 and canfieldite Ag_8SnS_6 measured at T = 295 K. The spectrum of Ag_8SnSe_6 consists of a single line with a linewidth of 0.93 mm/s. The Sn-119 spectrum of canfieldite Ag_8SnS_6, whose structural parameters and physical properties are known from the

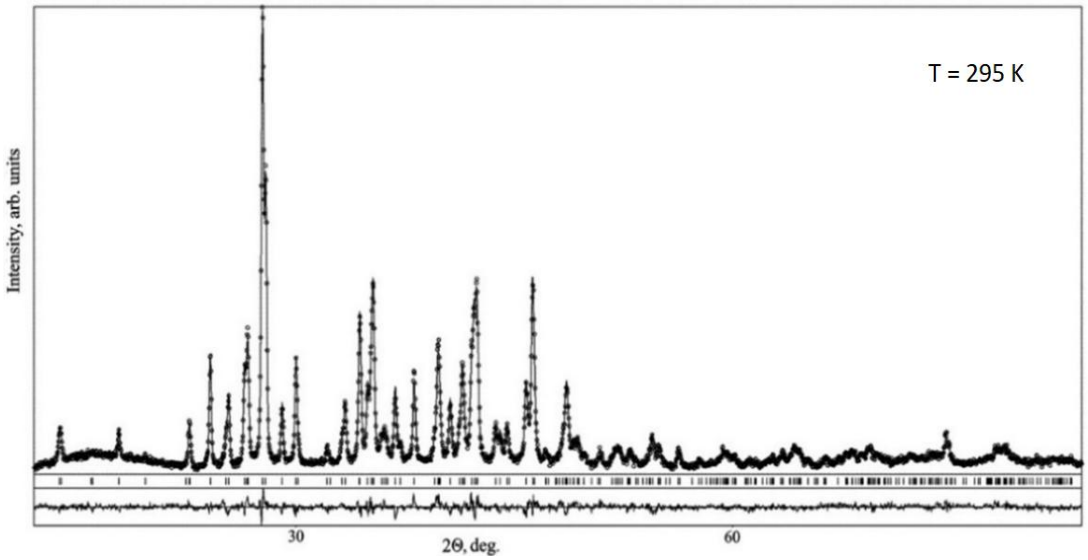

Fig.1. X-ray diffraction patterns of Ag_8SnSe_6 measured at T = 295 K.

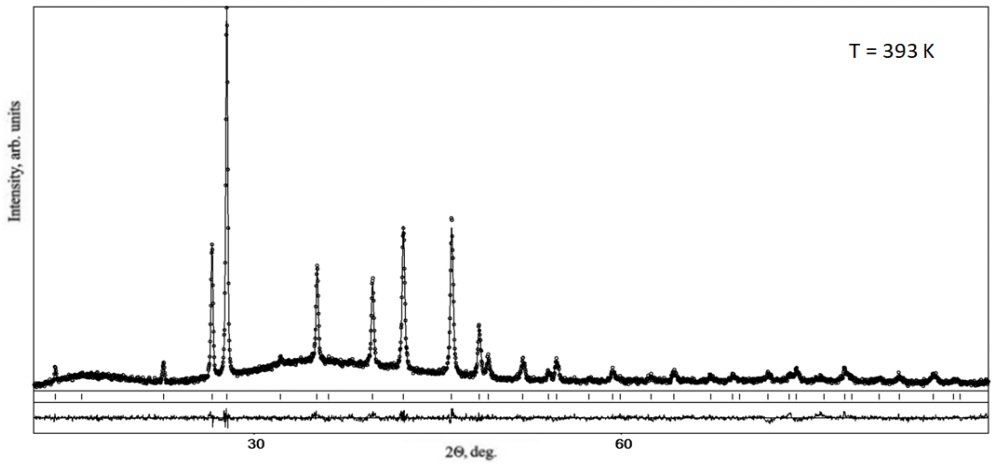

Fig.2. X-ray diffraction patterns of Ag8SnSe6 measured at T = 393 K.

Table 1.

The crystallographic parameters of Ag_8SnSe_6 argyrodite at T = 295 and 393 K

List	β′ - Ag_8SnSe_6 at T = 295 K	γ - Ag_8SnSe_6 at T = 393 K
Syngony and space group	Rhombic, Pnm21	Cubic, F $\overline{4}$ 3m
The lattice parameters, Å	a = 7.9165 (6) b = 7.8258 (7) c = 11.0534 (9)	a = 11.1230 (9)
The cell volume, Å^3	Vc = 684.8 (2)	Vc = 1376.1 (3)
The number of atoms in the cell	30.0 (two formula units)	61.2 (four formula units)
The number of Ag positions in the cell	7	3
Probability of filling partially vacant Ag positions	P = 0.921(7); 0.047(7); 0.102(8)	P = 0.324(3); 0.301(3); 0.068(2)
The number of Se atoms in the first coordination sphere relative to Sn	4	4
The number of Ag atoms in the second coordination sphere relative to Sn	18	60
Radius of the first coordination sphere, Å	2.60	2.48
Radius of the second coordination sphere, Å	4.06	3.98
Angles in Se-Sn-Se bonds	See Table 2	109.47°

Table 2.

Interatomic distances (Å) and bond angles (degrees) in the $SnSe_4$ tetrahedron for the β′ phase of Ag_8SnSe_6 (T = 295 K)

Bound	Distance, Å	Bound	Angle (degree)
Sn-Se(5)	2.482(11)	Se(5)-Sn-Se(5)	113.5(4)
Sn-Se(5)	2.482(11)	Se(5)-Sn-Se(4)	110.5(4)
Sn-Se(4)	2.525(13)	Se(5)-Sn-Se(3)	108.4(4)
Sn-Se(3)	2.584(14)	Se(5)-Sn-Se(4)	110.5(4)
		Se(4)-Sn-Se(3)	105.0(4)

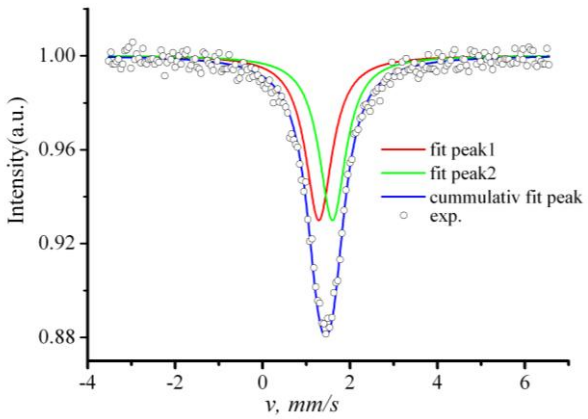

Fig. 3. Mössbauer spectrum of Sn^{119} in Ag_8SnSe_6 at T = 295 K.

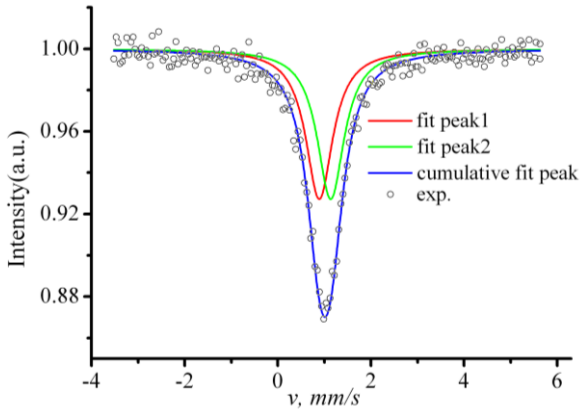

Fig. 4. Mössbauer spectrum of Sn^{119} in Ag_8SnS_6 at T = 295 K.

literature [20,21,22], exhibits a similar shape with a linewidth of 0.84 mm/s. Each spectrum is composed of a superposition of two quadrupole-split lines. The spectral parameters are summarized in Table 3, alongside corresponding literature data.

Table 3.

Isomer shifts (δ) (relative to SnO_2), quadrupole splitting (Δ) and spectral line widths ($G_1/_2$) for argyrodite and canfieldite at T = 295 K

Compound	δ, mm/s	Δ, mm/s	$G_{1/2}$, mm/s	Lit.
Ag_8SnSe_6	1.44	0.28	0.93	
	1.51	–	0.94	[23]
Ag_8SnS_6	1.01	0.22	0.84	
	1.52		1.03	[24]
	1.10	–	–	[25]

The obtained isomer shift values are characteristic of tetravalent tin [25]. The larger isomer shift for Sn-119 in Ag_8SnSe_6 compared to Ag_8SnS_6 indicates an increased 5s-electron charge density at the Sn-119 nuclei when transitioning from a tin environment coordinated by sulfur atoms (outer electron configuration $3s^23p^4$) to one coordinated by heavier chalcogen atoms, selenium (outer electron configuration $4s^24p^4$).

This increase in electron density may be attributed to enhanced covalency in the chemical bonds formed within the hybrid sp^3 orbitals characteristic of the tetrahedral sites [26] occupied by tin atoms in argyrodite and canfieldite. For both compounds, a moderate decrease in isomer shifts (δ) with increasing temperature (Fig. 5) was observed, indicating a reduction in electron density at the Sn nuclei and, presumably, its transfer to Ag atoms. This effect is expected to be accompanied by a decrease in the bond stiffness of Sn–X (X = S, Se) chemical bonds. The presence of such electron transfer is supported by data reported in [25], which showed that in solid solutions $Ag_{1-\gamma}Sn_{1+\gamma}Se_2$, the isomer shifts for Sn-119 nuclei increase as the number of Ag atoms surrounding the Sn atom decreases.

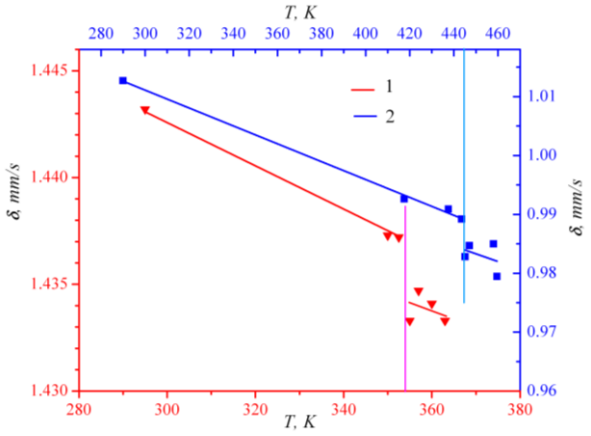

Fig. 5. Temperature dependence of isomer shifts for Sn-119 in argyrodite Ag_8SnSe_6 (1) and canfieldite Ag_8SnS_6 (2).

Quadrupole splittings observed in the spectra at T = 295 K (Figs. 3 and 4) are attributed to distortions of the local symmetry in the nearest environment of Sn atoms, leading to the appearance of electric field gradients (EFG) at the tin nuclei. At temperatures above the phase transitions (T = 356 K for Ag_8SnSe_6 and T = 445 K for Ag_8SnS_6), the spectral linewidths decrease: from 0.93 mm/s to 0.80 mm/s for argyrodite, and from 0.84 mm/s to 0.65 mm/s for canfieldite. This reduction is due to the local symmetry in both compounds becoming cubic, which results in a decrease or disappearance of the EFG. In the case of canfieldite, the linewidth at T = 445 K coincides with the instrumental linewidth. However, in argyrodite, inhomogeneity of the local electric fields at the tin nuclei persists in the γ phase.

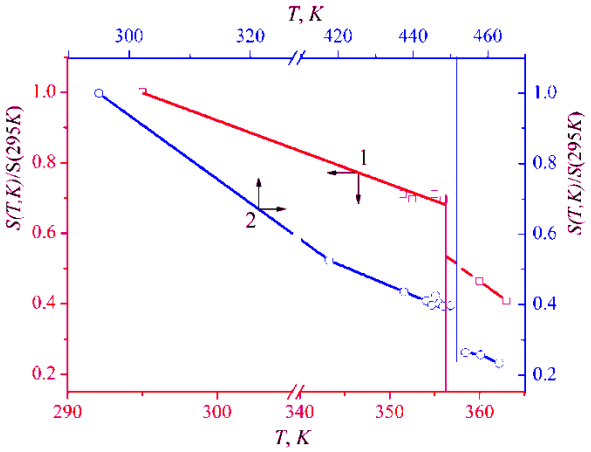

Fig. 6. Temperature dependence of the NGR spectral areas S for argyrodite Ag_8SnSe_6 (1) and canfieldite Ag_8SnS_6 (2), normalized to the values at T = 295 K.

To investigate the characteristics of the β′→γ phase transition in argyrodite Ag_8SnSe_6, NGR measurements were performed at fixed temperatures ranging from 351 to 363 K. A plot of the temperature dependence of the NGR spectral area normalized to the spectral area at T = 295 K, S(T)/S(295 K), was constructed (Fig. 6). For comparison, Fig. 6 shows a similar dependence for the related compound Ag_8SnS_6. The spectral area is proportional to the probability of the Mössbauer effect, which is given by the formula [27]:

$$f = \exp\left[-\frac{4\pi^2\langle x^2\rangle}{\lambda^2}\right],$$

where $\langle x^2\rangle$ is the mean square amplitude of the Sn-119 nucleus vibrations along the direction of gamma-ray emission.

As seen from the graphs of S(T)/S(295 K)$S(T)/S(295K)$, the probabilities of the Mössbauer effect on Sn-119 nuclei in both compounds sharply decrease near the temperatures of their phase transitions, β′→γ and α″→γ.

2.3. Sn atoms in argyrodite Ag_8SnSe_6 in the phase transition region and their coordination spheres

Figure 7 shows the "number-distance" histograms of Se and Ag atoms relative to the Sn atom in the argyrodite structure before (Fig. 7a) and after (Fig. 7b) the phase transition. The Se atoms (group 1, Fig. 7a) in the β′-Ag_8SnSe_6 structure (before the phase transition) form the

first coordination sphere with a radius of approximately 2.60 Å relative to the Sn atom, while the Ag atoms (group 2, Fig. 7a) form the second coordination sphere with a radius of approximately 4.06 Å (Table 1). The distance of 2.60 Å is comparable to the sum of the ionic radii of Sn^{4+} (0.74 Å) and Se^{2-} (1.91 Å), which totals 2.65 Å.

Thus, there is a possibility of overlap between the outer electron shells of Sn^{4+} and Se^{2-} ions and a transfer of electron charge density from selenium to tin, which accounts for the isomer shift value of 1.44 mm/s. The second coordination sphere, consisting of Ag atoms, does not directly affect the isomer shift of Sn-119 due to its considerable distance (the ionic radius of Ag^{+} is 1.26 Å).

The S^{2-} ions have a radius of 1.74 Å, which is smaller than that of Se^{2-}. Therefore, the overlap of their outer electron shells with those of Sn^{4+} (the sum of the ionic radii of Sn^{4+} and S^{2-} is 2.48 Å according to Pauling) [28] is less effective than in the case of Se^{2-}. As a result, the isomer shift value for α″-Ag_8SnS_6 δ = 1.01 mm/s) is lower compared to β′-Ag_8SnSe_6 (δ = 1.44 mm/s).

After the phase transition in argyrodite (T = 393 K), the Se atoms (group 1, Fig. 7b) form the first coordination sphere with a radius of 2.48 Å, and the Ag atoms (group 2, Fig. 7b) form the second coordination sphere with a radius of 3.98 Å (Table 1). However, this slight decrease in Sn–Se distances (0.12 Å) does not lead to an increase in the isomer shift, which, as seen in Fig. 5, sharply decreases during the phase transition. It should be noted that the same phenomenon is observed for canfieldite during its phase transition. By modeling, the spatial arrangement of Se atoms belonging to the first coordination sphere of Sn atoms and Ag atoms belonging to the second coordination sphere of Sn atoms was obtained, as shown in Fig. 8.

Based on the experimental data (Fig. 5), it can be concluded that the abrupt decrease in the isomer shift δ during the phase transition in Ag_8SnSe_6 indicates a sharp reduction in the electron density transferred to the outer s-shells of Sn from selenium atoms. Simultaneously, a different decrease in the NGR probability is observed, corresponding to an increase in the mean square displacements of Sn atoms (Fig. 6). This correlation can be explained by the influence of the second coordination sphere formed by Ag atoms. After the β′→γ phase transition, the number of bonds between selenium and silver atoms in the second coordination sphere increases more than threefold, from n2β′=18 to n2γ=60 (Table 1, Fig. 8). Since the distance between the first and second coordination spheres is 1.5 Å (Table 1), which is significantly less than the sum of the ionic radii of Se^{2-} (1.91 Å) and Ag^{+} (1.26 Å), it can be assumed that there is a partial transfer of electron density from selenium atoms to silver atoms. Indirect evidence for this is provided by the results of [29], which show that Ag atoms in argyrodite Ag_8GeS_6 possess the unique ability to withdraw electrons

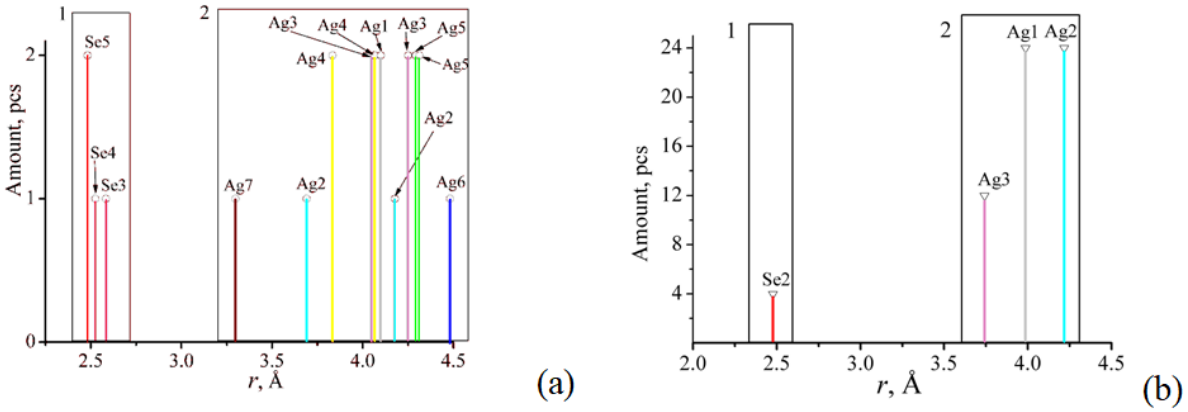

Fig. 7. "Number-distance" histogram of Se and Ag atoms relative to the Sn atom for the β′ (a) and γ (b) phases of Ag_8SnSe_6. 1 – group of Se atoms in the first coordination sphere; 2 – group of Ag atoms in the second coordination sphere.

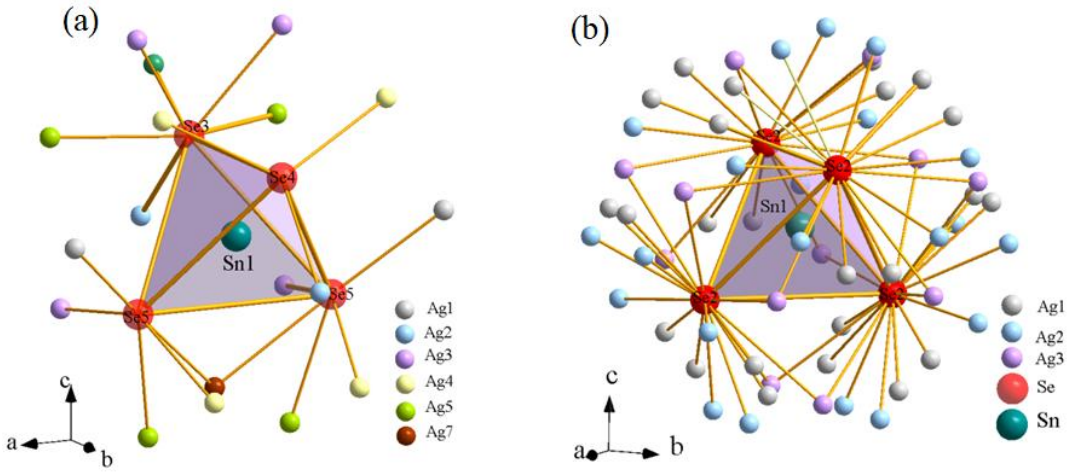

Fig. 8. Spatial models of the first and second coordination spheres of Sn- atoms in the β′- phase structure at T = 295 K (a) and γ- phase at T = 393 K (b) of Ag_8SnSe_6.

from the chalcogen S. This leads to a possible weakening of the Sn–Se bonds, resulting in an increase in the vibrational amplitude.

Conclusion

Using nuclear gamma resonance, the presence of phase transitions in argyrodite and canfieldite was confirmed at temperatures of 356 K and 445 K, respectively. It is shown that during the β′→γ phase transition in Ag_8SnSe_6 and the α′′→γ phase transition in Ag_8SnS_6, an abrupt increase in the root-mean-square vibrational amplitudes of Sn atoms occurs. It is hypothesized that an increase in Ag- site occupancy within the second coordination sphere of γ phase argyrodite influences the energy state of Sn nuclear levels, as evidenced by an abrupt change in isomer shift during the phase transition.

Quadrupole splittings and isomer shifts for Sn-119 atoms were measured in the β′ phase of Ag_8SnSe_6 and the α″ phase of Ag_8SnS_6. In the γ phase of Ag_8SnS_6, a homogeneous electric field at the tin nuclei is observed, whereas in the γ phase of Ag_8SnSe_6, possible electric field gradients associated with local distortions of the crystal lattice are present.

Histograms of "number-distance" distributions of Se and Ag atoms relative to the Sn atom were modeled for the β′ and γ phases of Ag_8SnSe_6. Spatial models of the first and second coordination spheres of Ag_8SnSe_6 in the β′ and γ modifications were proposed.

Chekailo M. V. – Candidate of Technical Sciences, Associate Professor of the Department of Physics;
Yushchuk S. I. – Doctor of Technical Sciences, Professor of the Department of Physics;
Yuryev S. O. – Candidate of Physical and Mathematical Sciences, Associate Professor of the Department of Physics;
Akselrud L. G. –Candidate of Chemical Sciences, Senior Researcher;
Mokliak V. V. – Doctor of Physical and Mathematical Sciences, Professor of the Department of Physical and Mathematical Sciences.

[1] Z. Zhang, Y. Shao, B. Lotsch *et al.*, *New horizons for inorganic solid state ion conductors*, Energy Environ. Sci. 11, 1945 (2018); https://doi.org/10.1039/C8EE01053F.
[2] J. B. Goodenough, *Fast Ionic Conduction in Solids*, in Physics and Chemistry of Electrons and Ions in Condensed Matter, edited by J. V. Acrivos, N. F. Mott, A. D. Yoffe, NATO ASI Series, Vol. 130, Springer, Dordrecht, 61 (1984); https://doi.org/10.1007/978-94-009-6440-2_61.
[3] F. Zheng, M. Kotobuki, S. Song, M. O. Lai, L. Lu, *Review on solid electrolytes for all-solid-state lithium batteries*, J. Mater. Chem. A 6, 1125 (2018); https://doi.org/10.1039/C7TA10584J.
[4] D. A. Weber, A. Senyshyn, K. S. Weldert et al., *Structural Insights and 3D Diffusion Pathways within the Lithium Superionic Conductor $Li_{10}GeP_2S_{12}$*, Chem. Mater. 28, 5905 (2016); https://doi.org/10.1021/acs.chemmater.6b02424.
[5] F. A. Karamov,*Superionic Conductors: Heterostructures and Elements of Functional Electronics Based on Them*, Cambridge Int Science Pub., Cambridge, U.K. (2008).
[6] L. Li, Y. Liu, J. Dai, A. Hong et al., *High thermoelectric performance of superionic argyrodite compound Ag_8SnSe_6*, J. Mater. Chem. C, 4, 5806 (2016); https://doi.org/10.1039/C6TC00810K.
[7] I. Valov, R. Waser, J. R. Jameson, M. N. Kozicki, *Electrochemical metallization memories—fundamentals, applications, prospects*, Nanotechnology, 22, 289502 (2011); https://doi.org/10.1088/0957-4484/22/28/289502.
[8] M. Yang, G. Shao, B. Wu, J. Jiang, S. Liu, L. Huimin, *Irregularly Shaped Bimetallic Chalcogenide Ag_8SnS_6 Nanoparticles as Electrocatalysts for Hydrogen Evolution*, ACS Appl. Nano Mater. 4, 6745 (2021); https://doi.org/10.1021/acsanm.1c00769.
[9] Y. Tingting, L. Li, Y. Zhang, *Recent progress in solid electrolytes for energy storage devices*, Adv. Funct. Mater. 30, 2000077 (2020); https://doi.org/10.1002/adfm.202000077.
[10] W.-Q. Hu, Y.-F. Shi, L.-M. Wu, *Synthesis and Shape Control of Ag_8SnS_6 Submicropyramids with High Surface Energy*, Cryst. Growth Des. 12, 3458 (2012); https://doi.org/10.1021/cg201649d.
[11] S. Lin, W. Li, Y. Pei, *Thermally insulative thermoelectric argyrodites*, Mater Today, 48, 198 (2021); https://doi.org/10.1016/j.mattod.2021.01.007.
[12] W. F. Kuhs, R. Nitsche, K. Scheunemann, *The argyrodites – a new family of tetrahedrally close-packed structures*, Mater. Res. Bull. 14, 241 (1979); https://doi.org/10.1016/0025-5408(79)90125-9.
[13] O. Gorochov, *Les composés Ag_8MX_6 (M = Si, Ge, Sn et X = S, Se, Te))*, Bull. Soc. Chim. Fr. 6, 2263 (1968).
[14] C. W. F. T. Pistorius, O. Gorochov, *Polymorphism and stability of the semiconducting series Ag_8MX_6 (M = Si, Ge, Sn, and X=S, Se, Te to high pressures*, *High Temp. - High Press.* 2, 39 (1970).
[15] M. V. Chekaylo, V. O. Ukrainets, G. A. Il'chuk, Y. P. Pavlovsky, N. A. Ukrainets, *Phase Transformations in the Charge at the Synthesis of Compounds of Argirodyte Family Ag_8XSe_6 (X = Si, Ge, Sn) (X = Si, Ge, Sn)*, Phys. Chem. Solid State, 12, 191 (2011).
[16] M. V. Chekaylo, V. O. Ukrainets, G. A. Ilchuk, N. A. Ukrainets, R. Y. Petrus, Ukrainian Patent No. 107754 (2015).
[17] L. Akselrud, Y. Grin, V. Pecharsky, P. Zavalij, B. Baumgartner, E. Wolfel, *Use of the CSD program package for structure determination from powder data*, Mater. Sci. Forum, 1, 335 (1993).

[18] M.V. Chekailo, L.G. Akselrud, R.E. Gladyshevskii, N.A. Ukrainets, *Temperature dependence of the structures of β′- and γ-Ag_8SnSe_6 argyrodite*, J. Solid State Chem. 332**,** 124541 (2024); https://doi.org/10.1016/j.jssc.2023.124541.
[19] K. Robinson, G. V. Gibbs, P. H. Ribbe, *Quadratic elongation: a quantitative measure of distortion in coordination polyhedra*, Science, 172**,** 567 (1971); https://doi.org/10.1126/science.172.3983.567.
[20] N. Wang, *New data for Ag_8SnS_6 (canfieldite) and Ag_8SnS_6 (argyrodite),* Neues Jahrb. Mineral. Monatsh. 6, 269 (1978).
[21] C.-L. Lu, L. Zhang, Y.-W. Zhang *et al.*, *Electronic, optical properties, surface energies and work functions of Ag_8SnS_6: First-principles method*, Chin. Phys. B, 24**,** 017501 (2015). https://doi.org/10.1088/1674-1056/24/1/017501.
[22] I.V. Semkiv, H.A. Ilchuk, N.Y. Kashuba, V.M. Kordan, A.I. Kashuba, *Synthesis, crystal and energy structure of the Ag_8SnS_6 crystal*, Phys. Chem. Solid State, 24, 441 (2023); https://doi.org/10.15330/pcss.24.3.441-447.
[23] M. Katada, *Mössbauer effect of 119/Sn in tin sulfides and their related compounds*, J. Sci. Hiroshima Univ. Ser. A-II, 39, 45 (1975).
[24] D. L. Smith, J. J. Zuckerman, *^{119m}Sn Mössbauer spectra of tin-containing minerals*, *J. Inorg. Nucl. Chem.* 29, 1203(1967); https://doi.org/10.1016/0022-1902(67)80358-0.
[25] F.S. Nasredinov, S.A. Nemov, V.F. Masterov, P.P. Seregin, *Mössbauer studies of two-electron tin centers with negative correlation energy in lead chalcogenides*, Solid State Phys. 41, 1897 (1999); https://doi.org/10.1134/1.1131091.
[26] I. B. Bersuker, *Structure and Properties of Coordination Compounds*, Khimiya, Leningrad (1971).
[27] G. K. Wertheim, *The Mössbauer Effect, Principles and Applications*, Academic Press, New York (1964).
[28] L. Pauling, *The Nature of the Chemical Bond and the Structure of Molecules and Crystals: An Introduction to Modern Structural Chemistry*, 3rd ed., Cornell University Press, Ithaca, NY. (1960). https://archive.org/details/natureofthechemicalbondpauling
[29] D.I. Bletskan, I.P. Studenyak, V.V. Vakulchak *et al.*, *Electronic structure of Ag_8GeS_6*, Semicond. Phys. Quantum Electron. Optoelectron. 20**,** 19 (2017); https://doi.org/10.15407/spqeo20.01.019.

М. В. Чекайло[1], С. І. Ющук[1], С. О. Юр'єв[1], Л. Г. Аксельруд[2], В. В. Мокляк[3,4]

Фазові переходи в Ag_8SnSe_6 та Ag_8SnS_6: мессбауерівські та рентгенівські дослідження

[1] Національний університет "Львівська політехніка", кафедра фізики, Львів, Україна, serhii.o.yuriev@lpnu.ua; mykola.v.chekailo@lpnu.ua
[2] Львівський національний університет імені Івана Франка, кафедра неорганічної хімії, Львів, Україна, lev.akselrud@lnu.edu.ua;
[3] Інститут металофізики ім. Г.В. Курдюмова, НАН України, Київ, Україна, mvvmcv@gmail.com;
[4] Івано-Франківський національний технічний університет нафти і газу, Івано-Франківськ, Україна, volodymyr.mokliak@nung.edu.ua

Структурні перетворення, що супроводжують низькотемпературний фазовий перехід (ФП) β′→γ в аргіродиті Ag_8SnSe_6, що характеризується змішаною електронно-іонною провідністю, були досліджені за допомогою ядерного гамма-резонансу (ЯГР) та рентгенівської дифракції (РД). Паралельні мессбауерівські дослідження були проведені на структурно спорідненому канфілдиті Ag_8SnS_6. Різке зниження ймовірності ефекту Мессбауера та ізомерних зсувів спостерігалося в аргіродиті та канфілдиті поблизу 356 К та 445 К відповідно, що відповідає фазовим переходам у цих сполуках. Запропоновано просторові моделі першої та другої координаційних сфер Ag_8SnSe_6 у β′ та γ-модифікаціях.

Ключові слова: аргіродит, канфілдит, фазові переходи, суперіонні провідники.